Infrared Spectroscopic Studies of Binary Solutions of Nitric Acid and Water and Ternary Solutions of Nitric Acid, Sulfuric Acid, and Water at Room Temperature: Evidence for Molecular Nitric Acid at the Surface

Husheng Yang[†] and Barbara J. Finlayson-Pitts*

Department of Chemistry, University of California at Irvine, Irvine, California 92697-2025

Received: November 15, 2000; In Final Form: January 9, 2001

Evidence from surface tension, sum frequency, and molecular scattering measurements in other laboratories has suggested that molecular HNO_3 is present at the surface of concentrated binary HNO_3-H_2O and ternary $HNO_3-H_2SO_4-H_2O$ solutions. We report here direct infrared spectroscopic evidence for the presence of HNO_3 at the air interface with both types of solutions at room temperature. Both attenuated total reflectance (ATR) and single reflectance SR-FTIR were applied to HNO_3-H_2O solutions ranging from 0.9 to 40 mol % (0.5−15.7 M) and to ternary solutions containing a constant amount of H_2SO_4 (25 mol %) and increasing concentrations of nitric acid from 0 to 25 mol % and associated decreasing amounts of water from 75 to 50 mol %. ATR spectra are analogous to transmission spectra, while SR spectra are more sensitive to species at or near the air interface where reflection occurs. Comparison of the ATR and SR spectra of the most concentrated solutions clearly show molecular HNO_3 at or near the surface. Furthermore, the spectra suggest that for these more concentrated solutions, the major form of nitric acid in the HNO_3-H_2O solution is the monohydrate, $HNO_3 \cdot H_2O$, while in the $H_2SO_4-HNO_3-H_2O$ solution, it is the anhydrous form. The potential atmospheric implications are discussed.

Introduction

There is a great deal of current interest in heterogeneous reactions in the atmosphere and, in particular, their potential role in the chemistry of oxides of nitrogen in the troposphere.[1−4] The surfaces with which tropospheric gases collide include not only airborne particles but also building materials and biological surfaces, all of which have water films. Thus, reactions at the air−water interface and in thin water films[5] on surfaces may be important in tropospheric chemistry. Experimental evidence for unique chemistry occurring at solution interfaces has been obtained, for example, in studies of the kinetics of uptake and reaction of Cl_2 with solutions containing bromide ions.[6] Similarly, Knipping et al.[7] showed that OH radicals must react with chloride ions not only in the bulk solution of suspended concentrated NaCl particles, but also at the air−solution interface, generating Cl_2 at much lower acidities than are required for the bulk reaction.

Recent studies in this laboratory[5,8] showed that a reaction of gaseous NO with HNO_3 adsorbed on a "wet" silica plate of high surface area takes place at room temperature. Molecular nitric acid was identified on the surface by its infrared absorption band at 1677 cm^{-1}. The subsequent introduction of gaseous NO led to the loss of adsorbed HNO_3 and the formation of gaseous NO_2 and smaller amounts of HONO. Similar chemistry was observed[5] using a geometrically smooth borosilicate glass surface at 50% relative humidity (RH) but not at relative humidities of 0 or 20%. It is therefore of interest to understand the chemical and physical state of nitric acid at the air−water interface and in thin water films, to understand at the molecular level the mechanisms of such heterogeneous NO_x reactions.

Donaldson and Anderson[9] recently reported that the surface tension of sulfuric acid−water and pure water was lowered on addition of nitric acid. They attributed lowering of the surface tension to the presence of molecular nitric acid at the air−water interface. In addition, Schultz and co-workers[10] showed, using sum frequency generation (SFG), that the disruption of the surface water hydrogen-bonded network increased with the concentration of HNO_3 in bulk solution. They attributed this to nitric acid at the surface, although an infrared absorption band due to the H−O stretch of HNO_3 expected in the spectral region they measured was not observed. Nathanson and co-workers[11] reported that the gaseous acids HCl and HBr impinging on a supercooled D_2SO_4 acid surface undergo relatively little H → D exchange, 11 and 22%, respectively. However, when HNO_3 was used instead of HCl and HBr, an exchange of more than 95% was observed, along with a much longer residence time in/on the sulfuric acid. This again suggested a unique interaction for HNO_3 at the surface.

We report here the results of single reflectance SR-FTIR studies of binary solutions of nitric acid in water (HNO_3-H_2O), as well as ternary solutions of nitric acid, sulfuric acid, and water ($H_2SO_4-HNO_3-H_2O$) at room temperature. As discussed in more detail below, SR probes not only the surface but also the bulk below to depths of the order of micrometers, depending on the particular solution and frequency of the radiation. Since the signal decays exponentially with depth from the interface, signals due to species at the air−solution interface are relatively stronger. For comparison to the literature, attenuated total reflectance (ATR) spectra were also taken. These ATR spectra are similar to transmission spectra of bulk solutions.[12,13] Thus, differences between the SR and ATR spectra reflect primarily

* To whom correspondence should be addressed. E-mail: bjfinlay@uci.edu. Telephone: (949) 824-7670. Fax: (949) 824−3168.

[†] Current address: Department of Chemistry, University of Idaho, Moscow, ID 83844-2343.

10.1021/jp004224f CCC: $20.00
Published on Web 02/15/2001

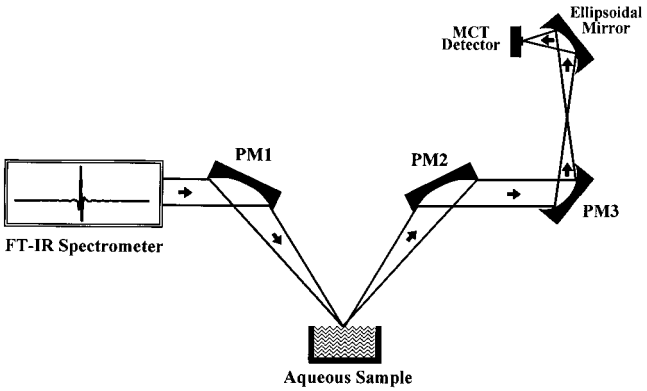

Figure 1. Schematic diagram of the SR-FTIR apparatus. PM1, PM2, and PM3 are aluminum off-axis parabolic mirrors. The sample cell was enclosed in a dry, nitrogen-purged box during the measurements.

differences in species at or near the interface. The results presented here provide direct spectroscopic evidence for the existence of surface HNO_3 proposed in the Donaldson and Anderson,[9] Schnitzer et al.,[10] and Morris et al.[11] studies. In addition, they suggest that at the interface of the concentrated HNO_3-H_2O solutions, nitric acid exists primarily as a monohydrate, while in the concentrated $H_2SO_4-HNO_3-H_2O$ solutions, it exists as anhydrous molecular HNO_3.

Experimental Section

1. Apparatus. Single reflectance spectra of HNO_3-H_2O and $HNO_3-H_2SO_4-H_2O$ solutions were measured using the apparatus shown in Figure 1. The external infrared beam from the FTIR spectrometer (Mattson GL-5020) was focused on the aqueous surface with an incident angle of 35° to the normal by an off-axis parabolic aluminum mirror (PM1). The beam reflected from the aqueous surface was captured by a second off-axis parabolic mirror (PM2), and then reflected to a third off-axis parabolic mirror (PM3). This directed the IR beam to a liquid nitrogen cooled MCT detector via an ellipsoidal mirror. The whole system was enclosed in a box which was purged with dry N_2 to reduce the contributions from gas-phase H_2O and CO_2 to the spectra. The aqueous surface was open to the N_2 purge during the measurements.

The intensity and shape of absorption bands in an SR spectrum depend on the angle of incidence and on the polarization.[14] We calculated the reflectance spectra of water using classical electromagnetic theory for both parallel and perpendicular polarization as described elsewhere,[14,15] and the optical constants of H_2O reported by Bertie and Lan.[16] Both spectra have the same shape at angles of incidence from 0 to 45°, encompassing the 35° used in these studies. As a result, a polarizer was not used in order to optimize the signal-to-noise ratio.

Transmission spectra were obtained by sandwiching the solutions between AgBr, NaCl, or ZnSe windows; the latter two were protected from the liquid by a thin Teflon film. While this was successful for a saturated $NaHSO_3$ solution used to test the comparison of different types of spectra, reproducibility problems were encountered for the strongly acidic solutions. Hence, for the acid solutions, we report here wavelength-corrected ATR spectra for comparison to the single-reflectance spectra.

ATR spectra were measured using a Tunnel cell (Axiom Analytical Incorporated, Irvine, CA) with an AMTIR crystal which was placed between the third parabolic mirror and the ellipsoidal mirror in Figure 1. Absorbance spectra were calculated by taking the ratio of a sample single-beam spectrum to the background single-beam spectrum of the empty ATR cell.

The binary HNO_3-H_2O and ternary $HNO_3-H_2SO_4-H_2O$ solutions were prepared by mixing 69.3 wt % HNO_3 (Fisher Scientific, ACS Certified Plus) and 96.0 wt % H_2SO_4 (Fisher Scientific, ACS Certified Plus) with 18 MΩ·cm water from a Barnstead/Nanopure Ultrapure Water System. The $NaHSO_3$ solution was prepared by dissolving the salt (Fisher Scientific, Certified ACS Grade) in Nanopure water.

2. ATR Data Analysis. ATR is an internal reflection technique in which light is directed into an infrared-transmitting crystal, which in this case is immersed in the acid solution. It strikes the interface at an angle greater than the critical angle and hence undergoes total internal reflection.[12,13] However, there is an evanescent wave that penetrates into the surrounding medium, with the depth of penetration depending on the angle of incidence and the indices of refraction of the crystal and the surrounding solution. As a result, if single-beam spectra with and without the absorbing species are ratioed, an absorption spectrum of the species can be obtained.

ATR spectra of bulk solutions are known to be very similar to transmission spectra, including following a Beer−Lambert type of relationship, but there are some differences.[12,13] For one particular angle of incidence and crystal-solution combination, the major factor is that the depth of penetration of the evanescent wave, and hence total absorption, varies directly with the wavelength (i.e., inversely with wavenumber). As a result, in bulk solutions the relative peak intensities using ATR decrease with increasing wavenumber in the infrared compared to those measured using a direct transmission cell. The position of peaks may also appear to have shifted slightly to shorter wavenumbers (up to ~10 cm^{-1}, depending on the angle of incidence), and for wide bands, broadening of the peak on the short wavenumber side is often seen.[12] The relative intensities for ATR spectra reported here have been corrected for the dependence on wavenumber by multiplying the measured absorbances by the wavenumber.

3. SR-FTIR Data Analysis. The SR spectra were analyzed in the following manner to obtain the absorption spectra. First, a reflectance spectrum ($R_{\bar{\nu}}$) was obtained by taking the ratio between a single-beam reflectance spectrum of the sample ($R^s_{\bar{\nu}}$) and that obtained by replacing the aqueous solution with a gold mirror ($R^{gm}_{\bar{\nu}}$), that is, $R_{\bar{\nu}} = R^s_{\bar{\nu}}/R^{gm}_{\bar{\nu}}$. In regions of strong light absorption, the refractive index (N) changes rapidly because of the contribution of the imaginary part, (k), due to absorption of light at that frequency:

$$N_{\bar{\nu}} = n_{\bar{\nu}} + ik_{\bar{\nu}} \qquad \text{(I)}$$

The reflectance spectrum contains information on the real part (n) of the refractive index of the liquid as a function of wavenumber ($\bar{\nu}$), as well as the imaginary part (k) when absorption of the light occurs. Absorption peaks in the reflectance mode typically appear as differential shaped peaks in the spectrum. The coefficient $k_{\bar{\nu}}$ of the imaginary part of the index of refraction is related to the absorption coefficient, $\sigma_{\bar{\nu}}$ at wavenumber $\bar{\nu}$ by eq II,

$$k_{\bar{\nu}} = \frac{C\sigma_{\bar{\nu}}}{4\pi\bar{\nu}} \qquad \text{(II)}$$

where C is the concentration of the absorbing species in molecule cm^{-3} and $\sigma_{\bar{\nu}}$ is the absorption coefficient in cm^2 $molecule^{-1}$. The absorption coefficient $\sigma_{\bar{\nu}}$ is proportional to $k_{\bar{\nu}}(\bar{\nu}) = k_{\bar{\nu}}(1/\lambda)$. For direct comparison to the ATR/transmission

spectra which are also proportional to $\sigma_{\bar{\nu}}$, the k spectra have been multiplied by wavenumber and the spectra scaled appropriately. The k spectra are therefore reported not in terms of, $k_{\bar{\nu}}$, but in terms of relative intensities which are proportional to $\sigma_{\bar{\nu}}$.

The Kramers−Kronig (KK) transform[17,18] was applied to the reflectance spectrum to obtain the absorption coefficient (k) spectrum as a function of wavenumber. The KK relationship relates the real and imaginary parts of the index of refraction using the measured reflectance spectrum, $R_{\bar{\nu}}$:

$$n_{\bar{\nu}} = \frac{1 - R_{\bar{\nu}}}{1 + R_{\bar{\nu}} - 2\cos\theta_{\bar{\nu}}\sqrt{R_{\bar{\nu}}}}$$
$$\mathrm{k}_{\bar{\nu}} = \frac{-2\sin\theta_{\bar{\nu}}\sqrt{\mathrm{R}_{\bar{\nu}}}}{1 + R_{\bar{\nu}} - 2\cos\theta_{\bar{\nu}}\sqrt{R_{\bar{\nu}}}} \qquad \text{(III)}$$

In equations (III), $\theta_{\bar{\nu}}$ is the phase shift angle given by

$$\theta_{\bar{\nu}_m} = \frac{2\bar{\nu}_m}{\pi}\int_0^{\infty}\frac{\ln(\sqrt{R_{\bar{\nu}}})d\bar{\nu}}{\bar{\nu}^2 - \bar{\nu}_m^2} \qquad \text{(IV)}$$

where $\bar{\nu}_m$ is the measured wavenumber. The integration is carried out in practice over a finite range of wavenumbers, $\bar{\nu}$, from 500 to 4000 cm^{-1}. KK transforms were performed using the IR/Raman application package provided by GRAMS/32 (Galactic Industries Corp., Salem, NH), which uses a double Fourier transform method to calculate the integrals.

Simulation of the SR-FTIR spectra at the air−water interface and calculation of the penetration depths as a function of wavenumber in water, the 40 mol % nitric acid solution and the H_2SO_4−HNO_3−H_2O solution containing 25 mol % each of HNO_3 and H_2SO_4 were performed using Matlab (The MathWorks, Inc., Nartic, MA). The program was originally written in FORTRAN code by Professor Richard A. Dluhy at the University of Georgia; we converted to Matlab functions for convenience of calculation. The real part (n) and imaginary part (k) of the refractive index for water were obtained from the literature.[16] The optical constants of the 40 mol % HNO_3 solution and the ternary solution were obtained by taking the KK transform of the SR-FTIR spectra measured using the apparatus in Figure 1. For air, n was taken as 1 and k as 0 at all wavenumbers. The penetration depths calculated using eq V

$$d_p = \frac{\lambda}{4\pi\cdot\mathrm{Im}(\sqrt{\hat{n}_2^{\,2} - \hat{n}_1^{\,2}\sin^2\theta})} \qquad \text{(V)}$$

in the region from 4000 to 500 cm^{-1} lie in the range from 0.7 to 90 μm, being smallest in the regions of water absorption, that is, ∼0.7 μm at 3414 cm^{-1} and 3−6 μm at 1638 cm^{-1}. In eq V, $\hat{n}_1$ and $\hat{n}_2$ are the complex refractive indexes of air and aqueous solution, and θ is the angle of incidence.

Comparison of Transmission/ATR and SR-FTIR Spectra. Ideally, if the composition of the surface is the same as the bulk, the absorption spectra obtained using transmission/ATR and SR should be identical. However, in practice, this is not the case, with potential deviations in both cases. For transmission/ATR spectra, there is a dispersion in the refractive index in the vicinity of an absorption band; this change in the refractive index causes changes in reflectivity losses which can be manifested in deviations from the true absorption spectrum.[12] In the case of the SR spectrum, deviations from the k-spectrum arise mainly from approximations in applying the KK transform. As discussed above, the KK transform involves the calculation of an integral from 0 to ∞ wavenumbers, but in practice, only a finite range of spectrum was measured (4000−500 cm^{-1} in our studies). To test for the effects of using a limited wavenumber region, we calculated the k-spectrum of a saturated $NaHSO_3$ solution using three wavenumber regions: 4000−500 cm^{-1}, 3000−500 cm^{-1}, and 1500−500 cm^{-1}, respectively. No significant differences in band shapes and positions were observed for the major bands of $NaHSO_3$ in the region from 1300 to 900 cm^{-1} except for a linear baseline change which can be easily corrected. Thus, the use of finite integration limits does not affect the calculated SR spectra. The KK transform also assumes normal incidence, while in our experiment, the angle of incidence is 35°; however, as discussed earlier, calculations for water show that the shape and position of the peaks is insensitive to angles up to ∼45°.

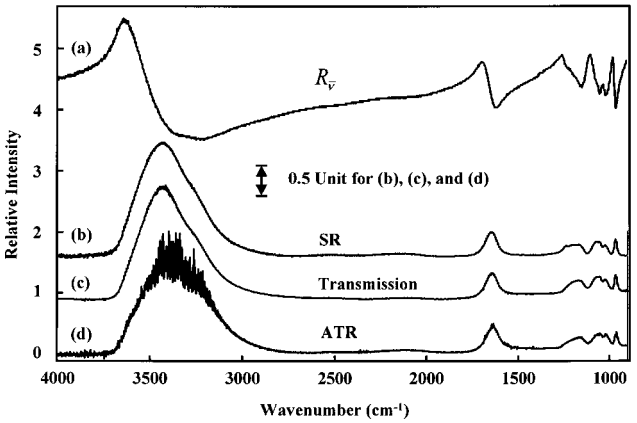

Figure 2. Comparison of SR and transmission spectra for a saturated $NaHSO_3$ solution. (a) Reflectance spectrum ($R_{\bar{\nu}}$) using a reflecting gold mirror for the background; (b) SR spectrum obtained by taking the KK transform of the reflectance spectrum, then multiplying the k-spectrum by wavenumber and scaling appropriately; (c) transmission spectrum with solution sandwiched between CaF_2 windows; (d) ATR spectrum.

To probe for such deviations, transmission and SR spectra were measured for a saturated solution of $NaHSO_3$. Figure 2a shows the reflectance spectrum as recorded, and Figure 2b shows the SR spectrum obtained by taking the KK transform of the reflectance spectrum, then multiplying the k-spectrum by wavenumber, and scaling appropriately. Figure 2c shows the transmission spectrum of the same solution held between CaF_2 windows, and Figure 2d, the ATR spectrum. As expected, absorption peaks in the transmission and ATR spectra appear in the reflectance spectrum (Figure 2a) as differential peaks. Comparison of the transmission and ATR spectra to the SR spectrum after the KK transform shows that they agree well, except for a small change in the baseline from 3000 to 2350 cm^{-1}, and a weak band at 1236 cm^{-1} in the SR spectrum. (The latter band occurs in all of our SR spectra, including neat H_2O, and appears to be an artifact due to aging of the gold surface used for the background spectra). The excellent agreement between the ATR/transmission and SR spectra establish that there are no anomalies that need to be taken into account in comparing these spectra for the acid solutions.

Results and Discussion

1. Spectra of Binary Solutions of HNO_3 and H_2O. Figures 3 and 4 show SR and ATR spectra of various solutions of nitric acid in water. Spectra (a) through (f) are in decreasing order of

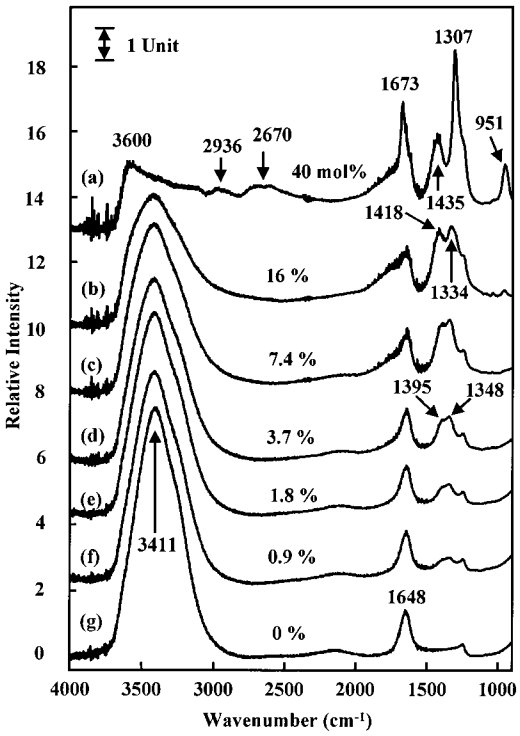

Figure 3. SR spectra of HNO_3-H_2O solutions. The concentrations of HNO_3 for spectra (a)−(f) are 40, 16, 7.4, 3.7, 1.8, and 0.9 mol %, respectively. Spectrum (g) is for pure water.

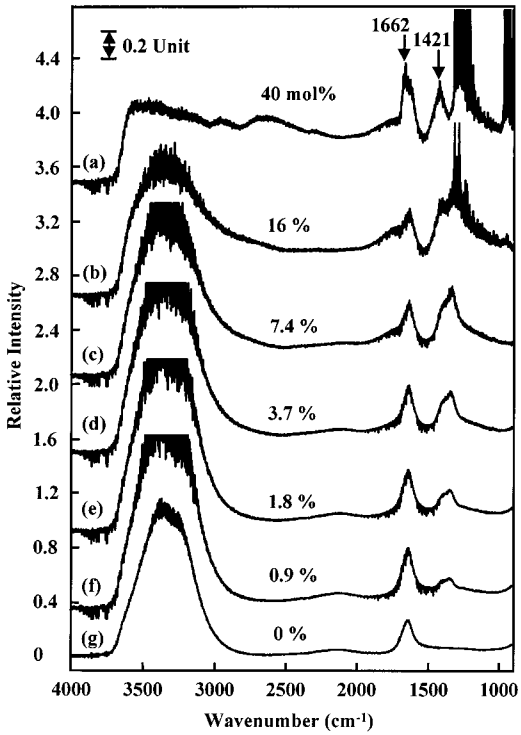

Figure 4. ATR spectra of the HNO_3 solutions shown in Figure 3.

concentration from 40 to 0.9 mol % HNO_3, while (g) is that for pure water. In both figures, absorption bands are observed in the most concentrated solutions at 951, 1307, 1435/1421, 1673/1662, 2670, and 2936 cm^{-1}; a broad peak is also seen at 3600 cm^{-1}. All but the latter peak are attributable to known absorption bands of molecular nitric acid: 2936 (2 ν_3), 2670 (2 ν_4), 1673 (ν_2), 1435 (ν_3), 1307 (ν_4), and 951 (ν_5).[19−22] It is interesting to note that the spectrum in Figure 3a corresponding to 40 mol % HNO_3 is very similar, especially in the region below 3000 cm^{-1}, to that reported for a solid amorphous thin film deposit of a 1:1 mixture of HNO_3:H_2O at lower temperatures and assigned to the monohydrate, $HNO_3 \cdot H_2O$.[20,21,23−25]

It is well-known that molecular nitric acid is largely undissociated at high concentrations. The degree of dissociation[26] of HNO_3 varies from 0.17 at 40 mol % to 0.99 at 0.9 mol % HNO_3. In addition, HNO_3 is known to form hydrates in these solutions, particularly the monohydrate and the trihydrate, with the relative amounts varying with the concentration of HNO_3 in solution.[27] At 40 mol %, for example, where the ratio of H_2O to HNO_3 is 3:2, the monohydrate $HNO_3 \cdot H_2O$ is the major form of the acid. Högefeldt[27] estimates that under these conditions, about 80% of the undissociated acid is in the form of the monohydrate, 12% is unhydrated HNO_3, and 8% is the trihydrate, $HNO_3 \cdot 3H_2O$. Hence, it is not surprising that the spectrum of the most concentrated solution is similar to that of the monohydrate at low temperatures.

In short, the infrared bands in the most concentrated solution are due to undissociated nitric acid hydrates, primarily the monohydrate. Ab initio calculations,[28] supported by microwave spectroscopic measurements,[29] show that when gas-phase HNO_3 forms a 1:1 complex with water, most of the infrared bands are shifted by relatively small amounts, <30 cm^{-1}. However, the H−O stretch of nitric acid is predicted to red-shift by ∼340 cm^{-1}, and the H−O−N bend is predicted to blue-shift by ∼150 cm^{-1}. While these calculations are for gaseous species, qualitatively similar shifts might be expected in solution for the undissociated, unhydrated form compared to that for the monohydrate. The red-shifted H−O stretch would be difficult to observe because of overlapping water bands (indeed, even the unshifted 3410 cm^{-1} band in liquid nitric acid is generally not observed for the same reason).[19] The H−O−N bend in gas-phase nitric acid[30] is at 1331 cm^{-1}, and in liquid HNO_3, it appears at 1395 cm^{-1}.[19] In HNO_3-H_2O solutions, this H−O−N bend is observed at ∼1430 cm^{-1}, blue-shifted by ∼100 cm^{-1} compared to that for the gas phase.[19] Such a shift is qualitatively consistent with the effects of hydrogen-bonding with water[31] and with the ab initio calculations.[28]

As the concentration is reduced below 40 mol % [spectra (b−f)], the peaks in the 1300−1500 cm^{-1} region change in a manner consistent with conversion of molecular nitric acid to the nitrate ion, that is, to the dissociated acid. The splitting of ∼130 cm^{-1} between the two bands at 1435 (ν_3) and 1307 (ν_4) cm^{-1}, characteristic of the monohydrate $HNO_3 \cdot H_2O$,[20,21,23−25] decreases and is replaced by a broad band at ∼1355 cm^{-1}. Comparisons to a SR spectrum of $NaNO_3$ and to literature spectra[32] show that this band is characteristic of the nitrate ion, NO_3^-, in aqueous solutions at room temperature. Simultaneously, the peak at ∼1670 cm^{-1} due to molecular nitric acid (Figures 3a and 4a) in the 40 mol % solution shifts toward lower wavenumbers and disappears into the peak at 1648 cm^{-1} due to liquid water. The same behavior has been reported in transmission studies of HNO_3-H_2O solutions at room temperature as well.[22]

In Figures 3 and 4, the absorption bands due to liquid water at ∼3400 and 1648 cm^{-1} are clearly visible in the spectra of the more dilute solutions. However, as the nitric acid concentration is increased to 40 mol %, the strongest water peak is shifted from 3400 cm^{-1} toward higher wavenumbers characteristic of non-hydrogen-bonded gas-phase water which has the ν_3 asymmetric stretch at 3756 and the ν_1 symmetric stretch at 3652 cm^{-1}.[33] This is reminiscent of recent studies of water adsorbed on NaCl[34] at submonolayer coverages which minimized lateral interactions associated with hydrogen bonding and led to a blue-

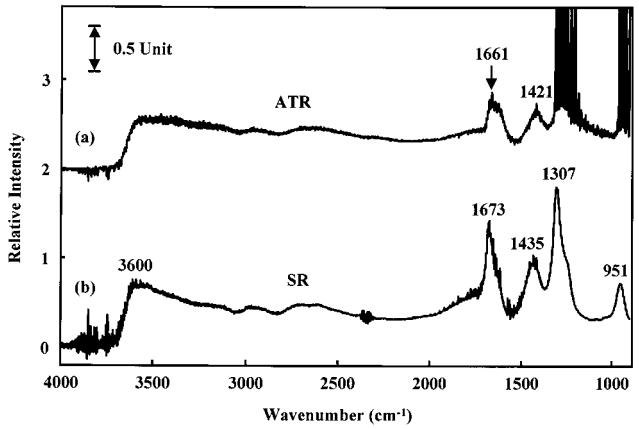

Figure 5. Comparison of the (a) ATR and (b) SR spectra of the 40 mol % HNO_3 solution. Spectrum (a) is the same as Figure 4a, and spectrum (b) is the same as Figure 3a.

shift in the 3400 cm^{-1} water band. In the present case of 40 mol % HNO_3, most of the water is tied up in the form of the hydrates as well as H_3O^+, whose ν_4 absorption band[19] at 1742 cm^{-1} can be seen as a broad shoulder on the high wavenumber side of the 1673 cm^{-1} nitric acid band. Thus, the amount of free, hydrogen-bonded liquid water is relatively small, resulting in a decrease in the 3400 cm^{-1} band and a shift of the remaining infrared absorption due to water to higher wavenumbers.

In short, the major features of both the SR and ATR spectra are consistent with nitric acid being primarily dissociated in the more dilute solutions, and changing to undissociated HNO_3 mainly in the form of the monohydrate, $HNO_3 \cdot H_2O$, in the most concentrated solution.

Figure 5 shows, however, that there are quantitative differences between the SR and ATR spectra of the most concentrated solution. In the SR-FTIR spectrum of pure water, the peak position of the water band in the 3700−3200 cm^{-1} region appears at 3410 cm^{-1}; this peak is blue-shifted to ∼3600 cm^{-1} both in the SR and ATR spectra shown in Figure 5. However, the 3600 cm^{-1} peak is more pronounced for the SR spectrum, suggesting less hydrogen-bonded liquid water in the surface film. In addition, the bands due to nitric acid at 1673, 1435, 1307, and 951 cm^{-1} are significantly more intense in the SR compared to the ATR spectrum. This comparison shows that molecular nitric acid must be enhanced at the surface of the most concentrated solution, since the contribution to absorption in SR spectra decreases exponentially with distance from the reflecting interface.

Because the ATR spectra have been corrected for the known wavelength dependence,[12,13] the actual ATR spectra as recorded had stronger bands in the lower wavenumber region. To ensure that an artifact is not introduced by correcting the absorbance for the wavelength dependence, the ATR and SR spectra for the 3.7 mol % (2 M) HNO_3 solution, where the nitric acid is 95% dissociated, were compared. As seen in Figure 6, the ATR-corrected relative band intensities in the 900−1700 cm^{-1} region, which are due to water at ∼1640 cm^{-1} and NO_3^- at 1355 cm^{-1}, are in excellent agreement with those in the SR spectrum. Hence, the less intense peaks in the ATR spectrum of the 40 mol % HNO_3 solution in Figure 5 cannot be an artifact from the wavelength correction.

This direct detection of the enhancement of HNO_3 at the interface is consistent with the surface tension measurements of Donaldson and Anderson[9] who proposed that the decrease in surface tension with increasing nitric acid concentrations was indicative of a surface film of HNO_3. Similarly, Shultz and co-

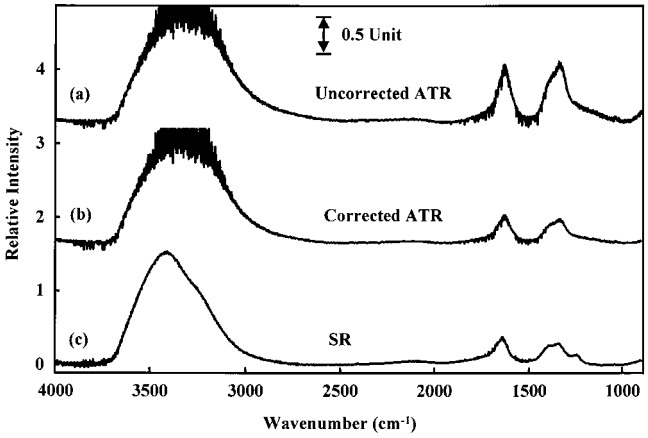

Figure 6. Comparison of the (a) ATR spectra for the 3.7 mol % HNO_3-H_2O solution as recorded; (b) corrected for the wavelength dependence; (c) the SR spectrum. The agreement of the relative band intensities between (b) and (c) supports the validity of the wavenumber correction to the ATR spectrum.

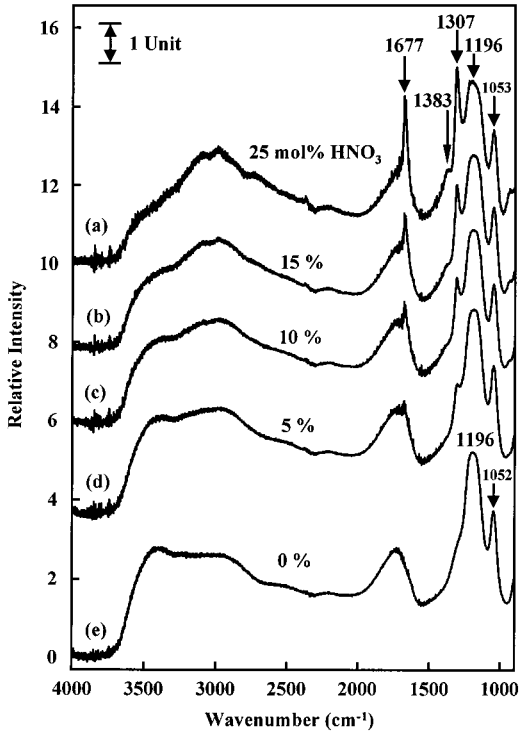

Figure 7. SR spectra of ternary solutions of $H_2SO_4-HNO_3-H_2O$. The mol % H_2SO_4 is 25% in all 5 solutions. The mol % HNO_3 is (a) 25, (b)15, (c) 10, (d) 5, and (e) 0.

workers[10] used SFG to show that, at 40 mol % HNO_3, there is no detectable signal from the dangling −OH of water at the surface and the signal from hydrogen-bonded water is very small. They attributed this to the formation of either contact ion pairs or molecular nitric acid at the surface, although a direct signal due to the H−O stretch in nitric acid expected in the spectral region they studied was not detected. The studies reported here appear to be the first direct detection of enhanced HNO_3 at the interface of these concentrated solutions.

2. Spectra of Ternary Solutions of HNO_3, H_2SO_4, and H_2O. Figure 7 shows a series of SR spectra of $H_2SO_4-HNO_3-H_2O$ solutions in which the mol % H_2SO_4 is constant at 25% and varying concentrations of HNO_3 from 25 mol % in part a to 0 mol % in part e are present. Bands due to molecular nitric acid at ∼1677, 1307, and 951 cm^{-1} are again clearly observed in the more concentrated solutions. The bands at ∼1196 and

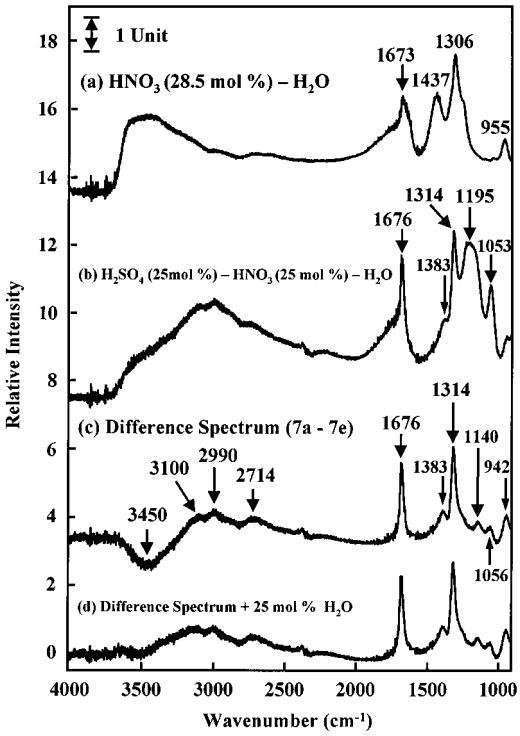

Figure 8. Comparison of SR spectra of (a) 28.5 mol % HNO_3-H_2O solution with (b) H_2SO_4 (25 mol %)$-HNO_3$ (25 mol %)$-H_2O$ (50 mol %) as in Figure 7a. The concentration of undissociated HNO_3 is the same in these two mixtures; (c) is the difference spectrum between H_2SO_4 (25 mol %)$-HNO_3$ (25 mol %)$-H_2O$ (50 mol %) and H_2SO_4 (25 mol %)$-H_2O$ (75 mol %), i.e. Figure 7a−e; (d) difference spectrum in (c) with one-third of water peak at 3400 cm^{-1} observed in Figure 7e added back to adjust for the different amounts of water in the subtracted spectrum.

1053 cm^{-1} seen both with and without HNO_3 are attributable to molecular H_2SO_4 and the bisulfate ion.[22] The spectra of both $H_2SO_4-H_2O$ as well as $H_2SO_4-HNO_3-H_2O$ are in agreement with spectra of such mixtures reported in the literature at room- and low temperatures.[22,35−40]

Figure 8 compares the SR spectra of a 28.5 mol % (12.3 M) HNO_3-H_2O solution (Figure 8a) to that of a ternary solution consisting of 25 mol % H_2SO_4, 25 mol % HNO_3, and 50 mol % H_2O; the HNO_3-H_2O solution is calculated to have the same concentration of undissociated nitric acid as in the $H_2SO_4-HNO_3-H_2O$ solution.[26] While molecular nitric acid bands are clear in both cases, there are several significant differences in the spectra of the two solutions.

These differences can be seen more clearly in Figure 8c which is the difference between the SR spectrum of the $H_2SO_4-HNO_3-H_2O$ solution (25:25:50%) and that of the $H_2SO_4-H_2O$ solution (25:75%). The bands due to sulfuric acid are subtracted out, but because there is more water in the $H_2SO_4-H_2O$ solution, the strong water band around 3400 cm^{-1} is over-subtracted, leading to a negative band in this region. However, comparison of the remaining absorption bands to those assigned to undissociated HNO_3 in Figure 8a show there is a red-shift in the 1437 cm^{-1} band, to 1383 cm^{-1} (the weak peaks at ∼1140 and 1056 cm^{-1} may be due to incomplete subtraction of the contributions from sulfate and bisulfate ions). This band is the H−O−N bend of nitric acid. The gas-phase fundamental for this bend appears at 1331 cm^{-1},[30] but consistent with the expected effects of hydrogen bonding on such a bending motion,[31] the infrared absorption is shifted to 1395 cm^{-1} in the pure liquid[19,41] and to 1429 cm^{-1} in water solutions.[19,22] The observation that the band is at ∼1383 cm^{-1} in the $H_2SO_4-HNO_3-H_2O$ solution suggests that the spectrum in Figure 8c is due to anhydrous, undissociated molecular nitric acid. This is consistent with the similarity of this spectrum to one of nearly anhydrous nitric acid particles at low temperatures (ref 21 and J. P. Devlin, personal communication).

Figure 8d shows the difference spectrum in Figure 8c but with the 3400 cm^{-1} water band corrected by an amount estimated to be equivalent to the 25 mol % difference in H_2O. It can be seen that there is then little in the way of absorption bands remaining in this region, in contrast to Figure 8a where a blue-shifted band assigned to water is evident. This is also consistent with the nitric acid at the surface being the anhydrous rather than the monohydrate form.

Thus, for the ternary solution, the surface is again enhanced in undissociated nitric acid. However, the position of the H−O−N bending vibration suggests that the form is anhydrous HNO_3, in contrast to the HNO_3-H_2O solution where the monohydrate appears to be the primary species. This may be due to the fact that H_2SO_4 is known to form acid hydrates which tie up the water.[42,43] For example, it has been found in SFG studies that, as the concentration of H_2SO_4 is increased, the signal from water at the interface decreases until there is essentially no signal due to water at sulfuric acid mole fractions ≥ 0.4.[44−47]

The presence of a film of anhydrous HNO_3 when added to $H_2SO_4-H_2O$ is consistent with the decreased surface tension of ternary solutions reported by Donaldson and Anderson[9] and with the results of molecular scattering experiments[11] which show that the residence time of HNO_3 on a D_2SO_4 surface is much longer than for HCl and HBr, allowing extensive H → D exchange to occur. It is interesting, however, that Fairbrother and Somorjai[48] also reported evidence for enhanced nitrogen at the surface of sulfuric acid, but only at temperatures below 200 K; in their studies, nearly anhydrous H_2SO_4 was used, in contrast to the other studies (including this one) where a substantial amount of water was present. In addition, the interface in their experiments was generated by exposing the initially pure sulfuric acid to gaseous nitric acid, whereas in the present studies and those of Donaldson and Anderson[9] a premixed ternary solution of nitric and sulfuric acids and water was used. Why either of these factors would result in different surface nitrogen enhancements at room temperature is not clear.

Atmospheric Implications. The studies reported here show that in concentrated binary HNO_3-H_2O and ternary $H_2SO_4-HNO_3-H_2O$ solutions, molecular HNO_3 is readily available at the air−solution interface. In the case of the binary solutions, the form of the nitric acid is primarily the monohydrate. However, when H_2SO_4 is present, water preferentially complexes with H_2SO_4, leaving anhydrous HNO_3 at the surface. The thermodynamics for heterogeneous reactions of nitric acid (which are potential "renoxification" routes),[5,8] and possibly the kinetics and mechanisms as well, may depend on the form of HNO_3 present at the surface. Studies are currently underway to explore any such differences. It is also possible that the health effects associated with inhaled particles, particularly highly acidic sulfate particles, are determined in part by the availability of the highly oxidizing nitric acid on the particle surface.

Acknowledgment. We are grateful to the California Air Resources Board for support of this work. We also thank M. J. Ezell, W. S. Barney, and T. Nordmeyer for assistance with setting up and testing the apparatus, and R. A. Dluhy, P. R. Griffiths, J. P. Devlin, G. E. Ewing, D. J. Donaldson, N. Saliba, and J. N. Pitts, Jr. for helpful discussions. We especially

appreciate R. A. Dluhy providing his programs for the calculation of infrared reflectance spectrum on an N-phase system of parallel, optically isotropic layers, and the calculation of the penetration depth in the last phase, G. Nathanson for providing a preprint prior to publication, and J. P. Devlin for providing unpublished spectra of anhydrous nitric acid.

References and Notes

(1) Finlayson-Pitts, B. J.; Pitts, J. N., Jr. *Chemistry of the Upper and Lower Atmosphere*; Academic Press: San Diego, 2000.

(2) de Reus, M.; Dentener, F.; Thomas, A.; Borrmann, S.; Strom, J.; Lelieveld, J. *J. Geophys. Res.* **2000**, *105*, 15.

(3) Dentener, F. J.; Carmichael, G. R.; Zhang, Y.; Lelieveld, J.; Crutzen, P. J. *J. Geophys. Res.* **1996**, *101*, 22.

(4) Raes, F.; VanDingenen, R.; Vignati, E.; Wilson, J.; Putaud, J.-P.; Seinfeld, J. H.; Adams, P. *Atmos. Environ.* **2000**, *34*, 4215.

(5) Saliba, N.; Mochida, M.; Finlayson-Pitts, B. J. *Geophys. Res. Lett.* **2000**, *27*, 3229.

(6) Hu, J. H.; Shi, Q.; Davidovits, P.; Worsnop, D. R.; Zahniser, M. S.; Kolb, C. E. *J. Phys. Chem.* **1995**, *99*, 8768.

(7) Knipping, E. M.; Lakin, M. J.; Foster, K. L.; Jungwirth, P.; Tobias, D. J.; Gerber, R. B.; Dabdub, D.; Finlayson-Pitts, B. J. *Science* **2000**, *288*, 301.

(8) Mochida, M.; Finlayson-Pitts, B. J. *J. Phys. Chem. A* **2000**, *104*, 9705.

(9) Donaldson, D. J.; Anderson, D. *Geophys. Res. Lett.* **1999**, *26*, 3625.

(10) Schnitzer, C.; Baldelli, S.; Campbell, D. J.; Shultz, M. J. *J. Phys. Chem. A* **1999**, *103*, 6383.

(11) Morris, J.; Behr, P.; Antman, M. D.; Ringeisen, B. R.; Splan, J.; Nathanson, G. M. *J. Phys. Chem. A* **2000**, *104*, 6738.

(12) Harrick, N. J. *Internal Reflection Spectroscopy*; Interscience Publishers: New York, 1967.

(13) Marley, N. A.; Gaffney, J. S.; Cunningham, M. M. *Spectroscopy* **1992**, *7*, 44.

(14) Dluhy, R. A.; Stephens, S. M.; Widayati, S.; Williams, A. D. *Spectrochim. Acta, Part A* **1995**, *51*, 1413.

(15) Dluhy, R. A. *J. Phys. Chem.* **1986**, *90*, 1373.

(16) Bertie, J. E.; Lan, Z. *Appl. Spectrosc.* **1996**, *50*, 1047.

(17) Krcho, D. "Kramers−Kronig Relations in Fourier Transform Infrared Spectroscopy of Semiconductors"; The 3rd Biennial Engineering Mathematics and Applications Conference, 1998, Adelaide, Australia.

(18) Ohta, K.; Ishida, H. *Appl. Spectrosc.* **1988**, *42*, 952.

(19) Querry, M. R.; Tyler, I. L. *J. Chem. Phys.* **1980**, *72*, 2495.

(20) Ritzhaupt, G.; Devlin, J. P. *J. Phys. Chem.* **1991**, *95*, 90.

(21) Devlin, J. P.; Uras, N.; Rahman, M.; Buch, V. *Isr. J. Chem.* **1999**, *39*, 261.

(22) Biermann, U. M.; Luo, B. P.; Peter, T. *J. Phys. Chem. A* **2000**, *104*, 783.

(23) Ritzhaupt, G.; Devlin, J. P. *J. Phys. Chem.* **1977**, *81*, 521.

(24) Tolbert, M. A.; Middlebrook, A. M. *J. Geophys. Res.* **1990**, *95*, 22423.

(25) Smith, R. H.; Leu, M.-T.; Keyser, L. F. *J. Phys. Chem.* **1991**, *95*, 5924.

(26) Davis, W. J.; DeBruin, H. J. *J. Inorg. Nucl. Chem.* **1964**, *26*, 1069.

(27) Högfeldt, E. *Acta Chem. Scand.* **1963**, *17*, 785.

(28) Tao, F.-M.; Higgins, K.; Klemperer, W.; Nelson, D. D. *Geophys. Res. Lett.* **1996**, *23*, 1797.

(29) Canagaratna, M.; Phillips, J. A.; Ott, M. E.; Leopold, K. R. *J. Phys. Chem. A* **1998**, *102*.

(30) McGraw, G. E.; Bernitt, D. L.; Hisatsune, I. C. *J. Chem. Phys.* **1965**, *42*, 237.

(31) Pimentel, G. C.; McClellan, A. L. *The Hydrogen Bond*; W. H. Freeman: San Francisco, 1960.

(32) Marley, N. A.; Gaffney, J. S.; Cunningham, M. M. *Environ. Sci. Technol.* **1993**, *27*, 2864.

(33) Herzberg, G. *Molecular Spectra and Molecular Structure. II. Infrared and Raman Spectra of Polyatomic Molecules*; D. Van Nostrand Company, Inc.: Princeton, New Jersey, 1945; Vol. II.

(34) Foster, M. C.; Ewing, G. E. *J. Chem. Phys.* **2000**, *112*, 6817.

(35) Adams, R. W.; Downing, H. D. *J. Opt. Soc. Am. A* **1986**, *3*, 22.

(36) Middlebrook, A. M.; Iraci, L. T.; McNeill, L. S.; Koehler, B. G.; Wilson, M. A.; Saastad, O. W.; Tolbert, M. A. *J. Geophys. Res.* **1993**, *98*, 20473.

(37) Anthony, S. E.; Tisdale, R. T.; Disselkamp, R.; Tolbert, M. A. *Geophys. Res. Lett.* **1995**, *22*, 1105.

(38) Iraci, L. T.; Middlebrook, A. M.; Tolbert, M. A. *J. Geophys. Res.* **1995**, *100*, 20969.

(39) Bertram, A. K.; Patterson, D. D.; Sloan, J. J. *J. Phys. Chem.* **1996**, *100*, 2376.

(40) Anthony, S. E.; Onasch, T. B.; Tisdale, R. T.; Disselkamp, R. S.; Tolbert, M. A. *J. Geophys. Res.* **1997**, *102*, 10777.

(41) Cohn, H.; Ingold, C. K.; Poole, H. G. *J. Chem. Soc.* **1952**, 4272.

(42) Wagman, D. D.; Evans, W. H.; Parker, V. B.; Schumm, R. H.; Halow, I.; Balley, S. M.; Churney, K. L.; Nuttall, R. L. *J. Phys. Chem. Ref. Data* **1982**, *11, Suppl. No. 2*.

(43) Phillips, L. F. *Aust. J. Chem.* **1994**, *47*, 91.

(44) Baldelli, S.; Schnitzer, C.; Shultz, M. J.; Campbell, D. J. *J. Phys. Chem. B* **1997**, *101*, 10435.

(45) Baldelli, S.; Schnitzer, C.; Shultz, M. J.; Campbell, D. J. *Chem. Phys. Lett.* **1998**, *287*, 143.

(46) Baldelli, S.; Schnitzer, C.; Campbell, D. J.; Shultz, M. J. *J. Phys. Chem. B* **1999**, *103*, 2789.

(47) Radüge, C.; Pflumio, V.; Shen, Y. R. *Chem. Phys. Lett.* **1997**, *274*, 140.

(48) Fairbrother, D. H.; Somorjai, G. A. *J. Phys. Chem. B* **2000**, *104*, 4649.